

# Nonlinear viscoelastic analysis of orthotropic beams using a general third-order theory

Venkat Vallala<sup>a</sup>, Annie Ruimi<sup>b</sup>, J.N. Reddy<sup>a,\*</sup>

<sup>a</sup>Advanced Computational Mechanics Laboratory, Department of Mechanical Engineering, Texas A&M University, College Station, TX 77843-3123, USA

<sup>b</sup>Department of Mechanical Engineering, Texas A&M University at Qatar, Education City, Doha, Qatar

## ARTICLE INFO

### Article history:

Available online 20 June 2012

### Keywords:

Finite element model  
Spectral/hp approximations  
General third-order beam theory  
Viscoelastic behavior  
von Kármán nonlinearity

## ABSTRACT

The displacement based finite element model of a general third-order beam theory is developed to study the quasi-static behavior of viscoelastic rectangular orthotropic beams. The mechanical properties are considered to be linear viscoelastic in nature with a scope to undergo *von Kármán* nonlinear geometric deformations. A differential constitutive law is developed for an orthotropic linear viscoelastic beam under the assumptions of plane-stress. The fully discretized finite element equations are obtained by approximating the convolution integrals using a trapezoidal rule. A two-point recurrence scheme is developed that necessitates storage of data from the previous time step only, and not from the entire deformation history. Full integration is used to evaluate all the stiffness terms using spectral/hp lagrange polynomials. The Newton iterative scheme is employed to enhance the rate of convergence of the nonlinear finite element equations. Numerical examples are presented to study the viscoelastic phenomena like creep, cyclic creep and recovery for thick and thin beams using classical mechanical analogues like generalized *n*-parameter Kelvin-Voigt solids and Maxwell solids.

© 2012 Elsevier Ltd. All rights reserved.

## 1. Introduction

### 1.1. Background

In the practical design and analysis of engineering structures, it becomes very important to predict the deflections, strains and stresses to prevent a catastrophic failure. If these are made of viscoelastic materials, then it becomes critical to evaluate the response of the structure over a long period. Experimental methods to measure these are often costly, time consuming and sometimes not possible. The theoretical and mathematical background of viscoelasticity has long been established [1–7]. Most of the analytical methods use the correspondence principle [8], to analyze viscoelastic problems. However, this method is restricted to very limited problems with simple geometry and loadings for which explicit solutions are available.

Hence, for practical design of viscoelastic structures there is a need for numerical methods like the finite element method [9], or the boundary element method [10]. The finite element method is a proven technique and has been applied to static and dynamic problems in structural mechanics. Most of the finite element approaches are based on integral transform methods [11], or superposition methods [12]. However, as noted by Chen and Lin [13],

these methods based on integral transforms, introduce errors into the numerical scheme, due to the approximate nature of the inversion techniques. They presented an incremental based finite element technique for the dynamic response of viscoelastic beams. It avoids the integral transformation, and thus the errors, by replacing the creep strain increments by fictitious body forces.

The early viscoelastic finite element codes are based on history integral forms, as in Ref. [14,15]. Finite element techniques based on these methods requires the storage of solution vector for the entire deformation history, which becomes a bottle neck when the computational memory is scarce. Johnson et al. [16] developed a technique based on differential constitutive law; Payette and Reddy [17] and Vallala et al. [18] developed a similar technique based on a two-point recurrence scheme. In the finite element formulations based on these, the data storage can be limited to the last few desired history steps. These formulations make use of mechanical analogues like spring and dashpots for the mathematical model, to predict the response of the viscoelastic structures. The classical generalized models of Maxwell solids, Maxwell-Voigt solids and *n*-parameter Kelvin-Voigt solids are used the most.

In this paper, a differential constitutive law is derived based on an assumed kinematic field (presented in the next section) that necessitates the use of 2D plane-stress constitutive model. The constitutive relations for linear anisotropic viscoelastic materials are given in Ref. [19,20]. We make use of fact that relaxation moduli for a linear orthotropic material is symmetric as verified exper-

\* Corresponding author. Tel.: +1 979 862 2417; fax: +1 979 845 3081.

E-mail addresses: [pradeepvv82@tamu.edu](mailto:pradeepvv82@tamu.edu) (V. Vallala), [annie.ruimi@qatar.tamu.edu](mailto:annie.ruimi@qatar.tamu.edu) (A. Ruimi), [jnreddy@tamu.edu](mailto:jnreddy@tamu.edu) (J.N. Reddy).

Report Documentation Page					
Public reporting burden for the collection of information is estimated to average 1 hour per response, including the time for reviewing instructions, searching existing data sources, gathering and maintaining the data needed, and completing and reviewing the collection of information. Send comments regarding this burden estimate or any other aspect of this collection of information, including suggestions for reducing this burden, to Washington Headquarters Services, Directorate for Information Operations and Reports, 1215 Jefferson Davis Highway, Suite 1204, Arlington VA 22202-4302. Respondents should be aware that notwithstanding any other provision of law, no person shall be subject to a penalty for failing to comply with a collection of information if it does not display a currently valid OMB control number.					
1. REPORT DATE <b>2012</b>		2. REPORT TYPE		3. DATES COVERED <b>00-00-2012 to 00-00-2012</b>	
4. TITLE AND SUBTITLE <b>Nonlinear viscoelastic analysis of orthotropic beams using a general third-order theory</b>				5a. CONTRACT NUMBER	
				5b. GRANT NUMBER	
				5c. PROGRAM ELEMENT NUMBER	
6. AUTHOR(S)				5d. PROJECT NUMBER	
				5e. TASK NUMBER	
				5f. WORK UNIT NUMBER	
7. PERFORMING ORGANIZATION NAME(S) AND ADDRESS(ES) <b>Texas A&amp;M University, Department of Mechanical Engineering, Advanced Computational Mechanics Laboratory, College Station, TX, 77843</b>				8. PERFORMING ORGANIZATION REPORT NUMBER	
9. SPONSORING/MONITORING AGENCY NAME(S) AND ADDRESS(ES)				10. SPONSOR/MONITOR'S ACRONYM(S)	
				11. SPONSOR/MONITOR'S REPORT NUMBER(S)	
12. DISTRIBUTION/AVAILABILITY STATEMENT <b>Approved for public release; distribution unlimited</b>					
13. SUPPLEMENTARY NOTES					
14. ABSTRACT <b>The displacement based finite element model of a general third-order beam theory is developed to study the quasi-static behavior of viscoelastic rectangular orthotropic beams. The mechanical properties are considered to be linear viscoelastic in nature with a scope to undergo von K<sub>r</sub>m<sub>n</sub> nonlinear geometric deformations. A differential constitutive law is developed for an orthotropic linear viscoelastic beam under the assumptions of plane-stress. The fully discretized finite element equations are obtained by approximating the convolution integrals using a trapezoidal rule. A two-point recurrence scheme is developed that necessitates storage of data from the previous time step only, and not from the entire deformation history. Full integration is used to evaluate all the stiffness terms using spectral/hp lagrange polynomials. The Newton iterative scheme is employed to enhance the rate of convergence of the nonlinear finite element equations. Numerical examples are presented to study the viscoelastic phenomena like creep, cyclic creep and recovery for thick and thin beams using classical mechanical analogues like generalized n-parameter Kelvin-Voigt solids and Maxwell solids.</b>					
15. SUBJECT TERMS					
16. SECURITY CLASSIFICATION OF:			17. LIMITATION OF ABSTRACT <b>Same as Report (SAR)</b>	18. NUMBER OF PAGES <b>10</b>	19a. NAME OF RESPONSIBLE PERSON
a. REPORT <b>unclassified</b>	b. ABSTRACT <b>unclassified</b>	c. THIS PAGE <b>unclassified</b>			

imentally by Halpin and Pagano [20]. The time dependent relaxation moduli in the viscoelastic constitutive equation is expanded in a Prony series for the mechanical analogue models used. For more on the constitutive equations and the number of independent constants in compliance/relaxation tensor see Ref. [21].

## 1.2. Higher-order beam theories

Beams are structural elements whose length is large compared to their cross-sectional dimensions. They are supported at few points along the length, and subjected to forces that make the structure to stretch and bend. Theories that are used to study the response of beams under external loads are obtained by reducing the general three-dimensional elasticity problem through a series of assumptions concerning the kinematics of deformation and constitutive behavior. The kinematic assumptions exploit the fact that such structures do not experience significant strains or stresses associated with the thickness direction. Thus, the solution of the three-dimensional elasticity problem associated with a beam structure is reformulated in terms of displacements or stresses, whose form is presumed on the basis of an educated guess concerning the nature of the deformation.

Beam theories based on the assumed form of the displacement field are most popular. In these theories, the displacements are expanded in increasing powers of the thickness (or height) coordinate. The word “order” refers to the power of the thickness coordinate in the power series expansion of the displacement field. The cubic expansion of the displacement field is optimal because it gives quadratic variation of transverse shear strain and stress, and require no “shear correction factors” compared to the lower-order Timoshenko beam theory, where the transverse shear strain and stress are constant through the beam thickness.

In the context of higher-order theories, there is no beam theory that accounts for shear deformation while not requiring shear correction factors, material variation through the beam thickness, and geometric nonlinearity. This very fact motivated the present study. The objective of the current paper is to develop a general third-order beam theory that accounts for two-constituent material properties with von Kármán nonlinear strains to capture the bending-extensional coupling. Hence we consider displacement field of the form

$$\begin{aligned} u_1(x, z, t) &= u(x, t) + z\theta_x(x, t) + z^2\phi_x(x, t) + z^3\psi_x(x, t) \\ u_2(x, z, t) &= 0 \\ u_3(x, z, t) &= w_0(x, t) + z\theta_z(x, t) + z^2\phi_z(x, t) \end{aligned} \quad (1.1)$$

Then the nonzero von Kármán nonlinear strains are

$$\begin{aligned} \varepsilon_{xx} &= \left[ \frac{\partial u}{\partial x} + \frac{1}{2} \left( \frac{\partial w}{\partial x} \right)^2 \right] + z \frac{\partial \theta_x}{\partial x} + z^2 \frac{\partial \phi_x}{\partial x} + z^3 \frac{\partial \psi_x}{\partial x} \\ \gamma_{xz} &= \theta_x + \frac{\partial w}{\partial x} + z \left( 2\phi_x + \frac{\partial \theta_z}{\partial x} \right) + z^2 \left( 3\psi_x + \frac{\partial \phi_z}{\partial x} \right) \\ \varepsilon_{zz} &= \theta_z + 2z\phi_z \end{aligned} \quad (1.2)$$

The strain field can be expressed as

$$\begin{aligned} \varepsilon_{xx} &= \varepsilon_{xx}^{(0)} + z\varepsilon_{xx}^{(1)} + z^2\varepsilon_{xx}^{(2)} + z^3\varepsilon_{xx}^{(3)} \\ \gamma_{xz} &= \gamma_{xz}^{(0)} + z\gamma_{xz}^{(1)} + z^2\gamma_{xz}^{(2)} \\ \varepsilon_{zz} &= \varepsilon_{zz}^{(0)} + z\varepsilon_{zz}^{(1)} \end{aligned} \quad (1.3)$$

where

$$\varepsilon_{xx}^{(0)} = \frac{\partial u}{\partial x} + \frac{1}{2} \left( \frac{\partial w}{\partial x} \right)^2, \quad \varepsilon_{xx}^{(1)} = \frac{\partial \theta_x}{\partial x}, \quad \varepsilon_{xx}^{(2)} = \frac{\partial \phi_x}{\partial x}, \quad \varepsilon_{xx}^{(3)} = \frac{\partial \psi_x}{\partial x} \quad (1.4)$$

$$\varepsilon_{zz}^{(0)} = \theta_z, \quad \varepsilon_{zz}^{(1)} = 2\phi_z, \quad \gamma_{xz}^{(0)} = \theta_x + \frac{\partial w}{\partial x}, \quad \gamma_{xz}^{(1)} = 2\phi_x + \frac{\partial \theta_z}{\partial x}, \quad \gamma_{xz}^{(2)} = 3\psi_x + \frac{\partial \phi_z}{\partial x} \quad (1.5)$$

It must be noted that the assumed form of displacement field gives rise to nonzero strain on the top and bottom surfaces of the beam. Also, it can be shown that all other third-order and lower-order theories can be derived from this; hence, we call it a *general third-order beam theory*. More details on higher-order shear deformable theories can be found in noted works by Reddy [22–24].

## 2. Constitutive model

As shown above, the assumed displacement field makes the strain  $\varepsilon_{zz}$  to be nonzero, which necessitates us to consider a 2D plane-stress constitutive model. For a linear orthotropic material the relation between second Piola–Kirchhoff stress tensor, denoted by  $\sigma$  and reduced strain tensor  $\mathbf{E} \approx \boldsymbol{\varepsilon}$  is given by

$$\begin{aligned} \begin{Bmatrix} \sigma_{xx} \\ \sigma_{zz} \\ \sigma_{xz} \end{Bmatrix} &= \begin{bmatrix} Q_{11}(0) & Q_{13}(0) & 0 \\ Q_{13}(0) & Q_{33}(0) & 0 \\ 0 & 0 & Q_{55}(0) \end{bmatrix} \begin{Bmatrix} \varepsilon_{xx}(x, t) \\ \varepsilon_{zz}(x, t) \\ \gamma_{xz}(x, t) \end{Bmatrix} \\ &+ \int_0^t \begin{bmatrix} \dot{Q}_{11}(t-s) & \dot{Q}_{13}(t-s) & 0 \\ \dot{Q}_{13}(t-s) & \dot{Q}_{33}(t-s) & 0 \\ 0 & 0 & \dot{Q}_{55}(t-s) \end{bmatrix} \begin{Bmatrix} \varepsilon_{xx}(x, s) \\ \varepsilon_{zz}(x, s) \\ \gamma_{xz}(x, s) \end{Bmatrix} ds \end{aligned} \quad (2.1)$$

where  $Q_{ij}$  are the time independent, plane-stress reduced, elastic coefficients and  $\dot{Q}_{ij}$  are the monotonically decreasing functions of time that constitute the plane-stress reduced viscous coefficients. The elastic plane-stress coefficients are related to engineering material constants as

$$\begin{aligned} Q_{11}(0) &= \frac{E_x(0)}{1 - \nu_{xz}\nu_{zx}}, \quad Q_{13}(0) = \frac{\nu_{xz}E_z(0)}{1 - \nu_{xz}\nu_{zx}} = \frac{\nu_{zx}E_x(0)}{1 - \nu_{xz}\nu_{zx}} \\ Q_{33}(0) &= \frac{E_z(0)}{1 - \nu_{xz}\nu_{zx}}, \quad Q_{55}(0) = G_{xz}(0) \end{aligned} \quad (2.2)$$

the time dependent viscous stiffness values are

$$\begin{aligned} \dot{Q}_{11}(t-s) &= \frac{\dot{E}_x(t-s)}{1 - \nu_{xz}\nu_{zx}}, \quad \dot{Q}_{13}(t-s) = \frac{\nu_{xz}\dot{E}_z(t-s)}{1 - \nu_{xz}\nu_{zx}} = \frac{\nu_{zx}\dot{E}_x(t-s)}{1 - \nu_{xz}\nu_{zx}} \\ \dot{Q}_{33}(t-s) &= \frac{\dot{E}_z(t-s)}{1 - \nu_{xz}\nu_{zx}}, \quad \dot{Q}_{55}(t-s) = \dot{G}_{xz}(t-s) \end{aligned} \quad (2.3)$$

where  $E_x(t)$  and  $E_z(t)$  are the extensional relaxation moduli and  $G_{xz}(t)$  is the shear relaxation moduli. Where as  $\nu_{xz}$  and  $\nu_{zx}$  are the major and minor Poisson's ratios of the beam. The specific forms of  $E_x(t)$ ,  $E_z(t)$  and  $G_{xz}(t)$  will depend on the material model employed. In this study, we express each one of them using a Prony series of order  $n$  as

$$E(t) = E_0 + \sum_{l=1}^n E_l e^{-\frac{t}{\tau_l^E}}, \quad G(t) = G_0 + \sum_{l=1}^n G_l e^{-\frac{t}{\tau_l^G}} \quad (2.4)$$

The time derivative of the relaxation moduli can be expressed as

$$\dot{E}(t) = -\sum_{l=1}^n \frac{E_l}{\tau_l^E} e^{-\frac{t}{\tau_l^E}}, \quad \dot{G}(t) = -\sum_{l=1}^n \frac{G_l}{\tau_l^G} e^{-\frac{t}{\tau_l^G}} \quad (2.5)$$

It is important to note that in the integral constitutive equations given by Eq. (2.1) we assume that a discontinuity exists in the response only at  $t = 0$ . This Prony series representation of the viscoelastic relaxation moduli is critical in developing the recurrence scheme and to implement efficient temporal numerical integration algorithms of the viscoelastic constitutive equations.

## 3. Weak form and semi-discrete element model

### 3.1. Galerkin weak form

To derive equations of motion we use the Hamilton's principle (see Ref. [23]) in the undeformed configuration

$$\int_{t_1}^{t_2} [\delta K - (\delta U + \delta V)] dt = 0 \quad (3.1)$$

where  $\delta K$  is the virtual kinetic energy,  $\delta U$  is the virtual strain energy, and  $\delta V$  is the virtual work done by external forces. Evaluating each of these terms and performing the necessary integration-by-parts with respect to  $x$  and  $t$ , we obtain the following weak forms of the governing equations over a typical finite element  $\Omega^e = (x_a, x_b)$ :

$$0 = \int_{x_a}^{x_b} \left( m_0 \ddot{u} \delta u + m_1 \ddot{\theta}_x \delta u + m_2 \ddot{\phi}_x \delta u + m_3 \ddot{\psi}_x \delta u + M_{xx}^{(0)} \frac{\partial \delta u}{\partial x} - F_x \delta u \right) dx - \left[ M_{xx}^{(0)} \delta u \right]_{x_a}^{x_b} \quad (3.2)$$

$$0 = \int_{x_a}^{x_b} \left( m_0 \ddot{w} \delta w + m_1 \ddot{\theta}_z \delta w + m_2 \ddot{\phi}_z \delta w + M_{xx}^{(0)} \frac{\partial w}{\partial x} \frac{\partial \delta w}{\partial x} + M_{xz}^{(0)} \frac{\partial \delta w}{\partial x} - F_z \delta w \right) dx - \left[ M_{xx}^{(0)} \frac{\partial w}{\partial x} \delta w + M_{xz}^{(0)} \delta w \right]_{x_a}^{x_b} \quad (3.3)$$

$$0 = \int_{x_a}^{x_b} \left( m_1 \ddot{u} \delta \theta_x + m_2 \ddot{\theta}_x \delta \theta_x + m_3 \ddot{\phi}_x \delta \theta_x + m_4 \ddot{\psi}_x \delta \theta_x + M_{xx}^{(1)} \frac{\partial \delta \theta_x}{\partial x} + M_{xz}^{(0)} \delta \theta_x \right) dx - \left[ M_{xx}^{(1)} \delta \theta_x \right]_{x_a}^{x_b} \quad (3.4)$$

$$0 = \int_{x_a}^{x_b} \left( m_2 \ddot{u} \delta \phi_x + m_3 \ddot{\theta}_x \delta \phi_x + m_4 \ddot{\phi}_x \delta \phi_x + m_5 \ddot{\psi}_x \delta \phi_x + M_{xx}^{(2)} \frac{\partial \delta \phi_x}{\partial x} + 2M_{xz}^{(1)} \delta \phi_x \right) dx - \left[ M_{xx}^{(2)} \delta \phi_x \right]_{x_a}^{x_b} \quad (3.5)$$

$$0 = \int_{x_a}^{x_b} \left( m_3 \ddot{u} \delta \psi_x + m_4 \ddot{\theta}_x \delta \psi_x + m_5 \ddot{\phi}_x \delta \psi_x + m_6 \ddot{\psi}_x \delta \psi_x + M_{xx}^{(3)} \frac{\partial \delta \psi_x}{\partial x} + 3M_{xz}^{(2)} \delta \psi_x - f_x^{(3)} \delta \psi_x \right) dx - \left[ M_{xx}^{(3)} \delta \psi_x \right]_{x_a}^{x_b} \quad (3.6)$$

$$0 = \int_{x_a}^{x_b} \left( m_1 \ddot{w} \delta \theta_z + m_2 \ddot{\theta}_z \delta \theta_z + m_3 \ddot{\phi}_z \delta \theta_z + M_{xz}^{(1)} \frac{\partial \delta \theta_z}{\partial x} + M_{zz}^{(0)} \delta \theta_z - f_z^{(1)} \delta \theta_z \right) dx - \left[ M_{xz}^{(1)} \delta \theta_z \right]_{x_a}^{x_b} \quad (3.7)$$

$$0 = \int_{x_a}^{x_b} \left( m_2 \ddot{w} \delta \phi_z + m_3 \ddot{\theta}_z \delta \phi_z + m_4 \ddot{\phi}_z \delta \phi_z + M_{xz}^{(2)} \frac{\partial \delta \phi_z}{\partial x} + 2M_{zz}^{(1)} \delta \phi_z - f_z^{(2)} \delta \phi_z \right) dx - \left[ M_{xz}^{(2)} \delta \phi_z \right]_{x_a}^{x_b} \quad (3.8)$$

where  $(\delta u, \delta w, \delta \theta_x, \delta \phi_x, \delta \psi_x, \delta \theta_z, \delta \phi_z)$  are the respective virtual variations that can be viewed as the test functions, and  $m_i$  are the mass inertias defined by

$$[m_0, m_1, m_2, m_3, m_4, m_5, m_6] = \int_A \rho [1, z, z^2, z^3, z^4, z^5, z^6] dA \quad (3.9)$$

The various internal stress resultants are defined as

$$[M_{xx}^{(i)}, M_{zz}^{(i)}, M_{xz}^{(i)}] = \int_A [\sigma_{xx}, \sigma_{zz}, \sigma_{xz}] z^i dA \quad (3.10)$$

The terms  $F_x$  and  $F_z$  due to the external loads are given as

$$F_x = f_x^{(0)}, \quad F_z = f_z^{(0)} \Rightarrow f_x^{(i)} = \int_0^L z^i \bar{f}_x dA, \quad f_z^{(i)} = \int_0^L z^i \bar{f}_z dA \quad (3.11)$$

Here  $\bar{f}_x, \bar{f}_z$  denote the distributed axial load and transverse load about the  $y$  axis respectively. The variational problem for the general third-order beam can be stated as: find  $(u, w, \theta_x, \phi_x, \psi_x, \theta_z, \phi_z) \in H^1(\Omega) \times H^1(\Omega) \times H^1(\Omega) \times H^1(\Omega) \times H^1(\Omega) \times H^1(\Omega) \times H^1(\Omega)$  for all  $(\delta u, \delta w, \delta \theta_x, \delta \phi_x, \delta \psi_x, \delta \theta_z, \delta \phi_z) \in H^1(\Omega) \times H^1(\Omega) \times H^1(\Omega) \times H^1(\Omega) \times H^1(\Omega) \times H^1(\Omega) \times H^1(\Omega)$

$(\Omega)H^1(\Omega) \times H^1(\Omega) \times H^1(\Omega)$  such that the equations Eqs. (3.2)–(3.8) hold true, where  $H^m(\Omega)$  is the Sobolev space of order  $m$  and  $\Omega = [x_a, x_b]$ .

### 3.2. Semi-discrete finite element model

Since the assumed kinematic displacement requires only the continuity of the primary variables across the element boundaries and not its derivatives, i.e.,  $C^0$ -continuous, we use the following equal-order interpolation functions for all variables

$$[u(x, t), w(x, t), \theta_x(x, t), \phi_x(x, t), \psi_x(x, t), \theta_z(x, t), \phi_z(x, t)] = \sum_{j=1}^m [u_j(t), w_j(t), \theta_{xj}(t), \phi_{xj}(t), \psi_{xj}(t), \theta_{zj}(t), \phi_{zj}(t)] \psi_j(x) \quad (3.12)$$

where  $\psi_j$  are the one-dimensional nodal spectral interpolation functions. The nodal expansion in the interval  $\Omega_{st} = [-1, +1]$  for a typical finite element is defined as

$$\psi_j(\xi) = \frac{(\xi - 1)(\xi + 1)L_p^j(\xi)}{(p)(p + 1)L_p(\xi_j)(\xi - \xi_j)} \quad (3.13)$$

where  $L_p = P_p^{0,0}$  are the Legendre polynomials of order  $p$ , and  $\xi_j$  denotes the location of the roots of  $(\xi - 1)(\xi + 1)L_p^j(\xi) = 0$  in the interval  $[-1, +1]$ . These set of points  $\{\xi_j\}_{j=1}^{p+1}$  are commonly referred to as Gauss-Lobatto-Legendre (GLL) points. Other nodal bases like Chebyshev second-kind can also be used. The location of nodes in a typical master element coincides with the roots of Legendre polynomial hence the basis is called “spectral” [25]. In spectral basis the nodes are not equally spaced within the canonical interval  $[-1, +1]$ . At high polynomial orders (five and above) the equi-spaced interpolation functions exhibit spurious oscillations at the ends of the interval, this is called *Runge effect*. This impacts the accuracy and reliability of finite element formulation. The spectral nodal basis does not suffer from this and also the Kronecker delta property, i.e.,  $\psi_j(\xi_i) = \delta_{ij}$  is not compromised.

In Fig. 1a we can see Runge oscillations for equally spaced Lagrange basis near the ends of the interval and in Fig. 1b the cardinality condition of Kronecker delta is obvious. In generating the above plot and in our code an analytically less complex and computationally more stable form of Eq. (3.13) is used to generate the nodal basis. The equation is shown below

$$\psi_i(\xi) = \prod_{j=1, j \neq i}^{p+1} \frac{(\xi - \xi_i)}{(\xi_i - \xi_j)} \quad (3.14)$$

Multi-dimensional spectral interpolation functions can be obtained from the tensor product of the above one-dimensional equation [9,26]. Substituting Eq. (3.12) into the weak forms in Eqs. (3.2)–(3.8), yields the semi-discrete finite element model of the beam element. The quasi-static finite element equations can be expressed as (and are given explicitly in Appendix A)

$$\mathbf{K}\mathbf{\Lambda} + \int_0^t \tilde{\mathbf{K}}\mathbf{\Lambda}(s) ds = \mathbf{F} \quad (3.15)$$

## 4. Fully discretized finite element equations

### 4.1. Time discretization using recurrence formulation

In order to derive fully discretized finite element equations, we start with the partitioning of the time interval  $[0, T] \subset \mathbb{R}$  (region of interest) into set of  $N$  non-overlapping subintervals such that

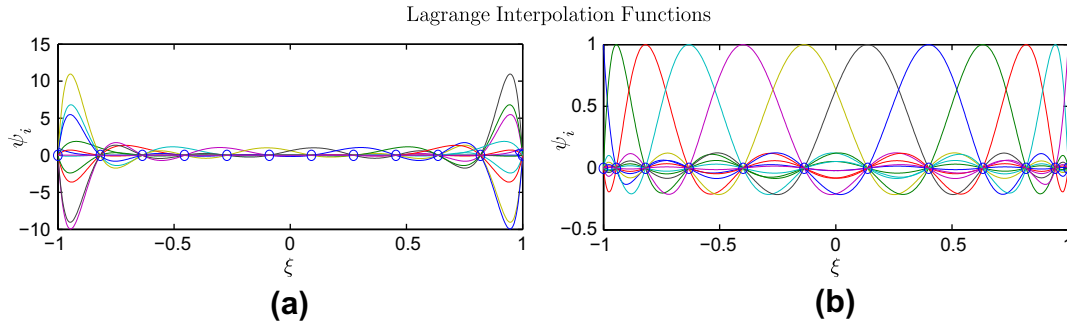


Fig. 1. Graphs of (a) equi-spaced and (b) spectral Lagrange interpolation functions for polynomial order of  $p = 11$ .

$$[0, T] = \bigcup_{k=1}^N [t_k, t_{k+1}] \quad (4.1)$$

The final solution is obtained by repeatedly solving an initial value problem within each subregion  $[t_k, t_{k+1}]$ , with the known values of solution at  $t = t_k$  as initial conditions. From Eq. (3.15) it is clear that the semi-discrete finite element equations have contributions from elastic and viscous parts of the constitutive relations. The elastic part is simple and straight forward, however, the contribution from viscous part is in the form of convolution integrals, hence the full discretization of these is not a trivial task. In order to solve the problem in each subinterval, we can approximate these convolution integrals using two-point (trapezoidal rule) or three-point (Simpson's rule) formulas. But a direct temporal integration from here, results in a computationally unattractive solution procedure which requires the storage of the entire deformation history. It becomes a bottle neck for storing these when the computational memory is scarce. Also, when the total number of time steps  $N$  is large, much of the computational time expended to get the solution at a subinterval, goes into the evaluation of the convolution integrals.

To circumvent these issues, we develop a recurrence scheme for two-point (trapezoidal rule) formula that can be used to approximate the convolution integrals within each subinterval. The two-point recurrence scheme requires the storage of the generalized displacements and a set of internal variables evaluated at the Gauss points, from the previous time step only. A similar three-point Simpson's scheme, which requires the storage from last two time steps, is used in Ref. [27]. Using these ideas, the convolution integral appearing in Eq. (3.15) can be expressed as

$$\int_0^{t_N} \tilde{\mathbf{K}} \Delta(s) ds = \sum_{k=1}^{N-1} \int_{t_k}^{t_{k+1}} \mathbf{K} \Delta(s) ds \quad (4.2)$$

In order to develop the recurrence formulation the following multiplicative decomposition of the relaxation moduli [28], is used. These equations hold true as the relaxation moduli can be expressed in terms of Prony series within each subinterval.

$$\begin{aligned} \dot{E}(t_{k+1} - s) &= \sum_{l=1}^n e^{-\Delta t_k / \tau_l^E} \dot{E}_l(t_k - s) \\ \dot{G}(t_{k+1} - s) &= \sum_{l=1}^n e^{-\Delta t_k / \tau_l^G} \dot{G}_l(t_k - s) \end{aligned} \quad (4.3)$$

where  $\Delta t_k = t_{k+1} - t_k$ . Using the above, Eq. (4.2) can be expressed in index notion at an arbitrary time step  $t = t_s$  as

$$X_i(t_s) = \sum_{k=1}^{s-1} \int_{t_k}^{t_{k+1}} \tilde{K}_{ij} \Delta_j(s) ds \cong \sum_{l=1}^n \sum_{m=1}^{NGP} \alpha_m \bar{X}_i^{lm}(t_s) \quad (4.4)$$

where Einstein's summation convention on repeated indices is implied. As noted previously, Gauss quadrature is employed in evaluation of  $\tilde{K}_{ij}$ , resulting in the summation over  $m$  (where NGP is the number of Gauss points). The quantity  $\bar{X}_i^{lm}$  assumes the following possible forms for extensional and shear moduli

$$\bar{X}_i^{lm}(t_s) = e^{-\frac{\Delta t_{s-1}}{\tau_l^E}} \bar{X}_i^{lm}(t_{s-1}) - \frac{\Delta t_{s-1}}{2} \frac{E_l}{\tau_l^E} \left( e^{-\frac{\Delta t_{s-1}}{\tau_l^E}} f_i^m(t_{s-1}) + f_i^m(t_s) \right) \quad (4.5)$$

$$\bar{X}_i^{lm}(t_s) = e^{-\frac{\Delta t_{s-1}}{\tau_l^G}} \bar{X}_i^{lm}(t_{s-1}) - \frac{\Delta t_{s-1}}{2} \frac{G_l}{\tau_l^G} \left( e^{-\frac{\Delta t_{s-1}}{\tau_l^G}} f_i^m(t_{s-1}) + f_i^m(t_s) \right) \quad (4.6)$$

Note to get the above expressions, we replaced convolution integrals with in each subinterval with a two-point trapezoidal rule. Also, the specific forms of  $\alpha_m$  and  $f_i^m(t_s)$  depend on components of  $\tilde{K}_{ij}$ . In Eq. (4.4), even though there are  $(s-1)$  time steps of  $k$  to get to time  $t = t_s$ , the above equations just need the values of solution  $\{\Delta(t_s)\}$  and internal variables  $\bar{X}_i^{lm}(t_{s-1})$  from  $k = t_s$  and  $k = t_{s-1}$ . There is no need to store these values for all the  $(s-1)$  time steps. Thus the above equations represent recurrence formulas in terms of the internal variables  $\bar{X}_i^{lm}(t_s)$  with  $\bar{X}_i^{lm}(t_1) = 0$ . Using Eqs. (4.5), (4.6) results in the following quasi-static fully-discretized equations for generalized displacements at the current time step (the components are presented in Appendix B)

$$[\bar{K}]_s \{\Delta(t_s)\} = \{F\}_s - \{\tilde{Q}\}_s \quad (4.7)$$

## 5. Numerical examples

In this paper, we make use of higher-order spectral interpolation functions without resorting to any selective or reduced integration techniques. The nonlinear finite element equations are linearized using Newton–Raphson's procedure (see Appendix B) and the equations are solved using an iterative scheme. Since a nonlinear beam becomes stiff with load, the total load is divided into smaller load steps, with the solution of each step being used for the next. For all the problems we use five load steps with a maximum of 10 nonlinear iterations at each step. All problems in this study converged within five iterations for a tolerance of  $\varepsilon = 10^{-6}$ . The computational domain is reduced by taking advantage of the symmetry of the beam about  $x = L/2$ . The boundary conditions considered in the analysis are.

### (1) Hinged at both ends:

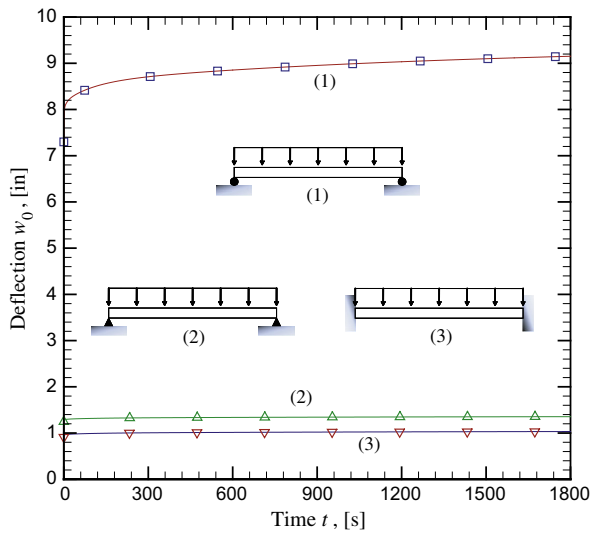
$$\begin{aligned} w(0) &= 0, \quad u(L/2) = 0, \quad \theta_x(L/2) = 0, \quad \phi_x(L/2) \\ &= 0, \quad \psi_x(L/2) = 0 \end{aligned} \quad (5.1)$$

### (2) Pinned at both ends:

$$\begin{aligned} u(0) &= 0, \quad w(0) = 0, \quad u(L/2) = 0, \quad \theta_x(L/2) \\ &= 0, \quad \phi_x(L/2) = 0, \quad \psi_x(L/2) = 0 \end{aligned} \quad (5.2)$$

**Table 1**  
Viscoelastic moduli.

$E_0$	205.7818 Ksi		
$E_1$	43.1773 Ksi	$\tau_1^E$	$9.1955 \times 10^{-1}$ s
$E_2$	9.2291 Ksi	$\tau_2^E$	$9.8120 \times 10^0$ s
$E_3$	22.9546 Ksi	$\tau_3^E$	$9.5268 \times 10^1$ s
$E_4$	26.2647 Ksi	$\tau_4^E$	$9.4318 \times 10^2$ s
$E_5$	34.6298 Ksi	$\tau_5^E$	$9.2066 \times 10^3$ s
$E_6$	40.3221 Ksi	$\tau_6^E$	$8.9974 \times 10^4$ s
$E_7$	47.5275 Ksi	$\tau_7^E$	$8.6852 \times 10^5$ s
$E_8$	46.8108 Ksi	$\tau_8^E$	$8.5142 \times 10^6$ s
$E_9$	58.6945 Ksi	$\tau_9^E$	$7.7396 \times 10^7$ s

**Fig. 2.** Quasi-static maximum vertical deflection  $w_{max}$ , of viscoelastic beam under uniform distributed load  $q$ .**Table 2**

Quasi-static finite element results for the maximum deflection  $w_{max}$  of a viscoelastic beam under uniform distributed load  $q$  with three different sets of boundary conditions.

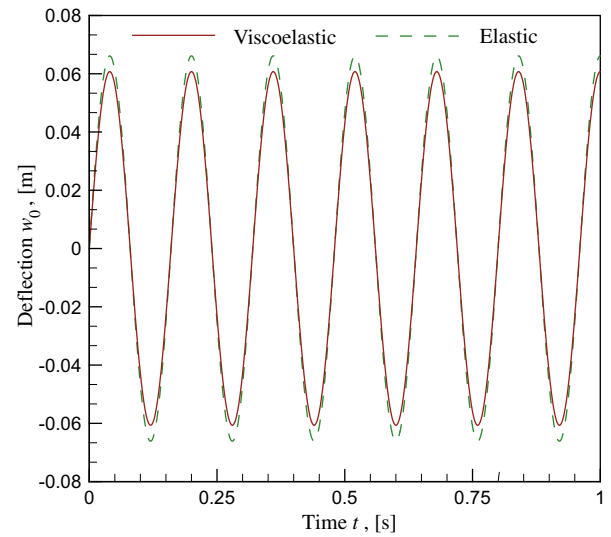
Time, $t$	Flügge	$\Delta t = 0.1$	$\Delta t = 0.5$	$\Delta t = 1.0$	$\Delta t = 2.0$
0	7.2980	7.2995	7.2995	7.2995	7.2995
200	8.5429	8.5457	8.5648	8.6237	8.8512
400	8.6827	8.6856	8.7052	8.7661	9.0014
600	8.7680	8.7710	8.7910	8.8531	9.0931
800	8.8364	8.8394	8.8597	8.9228	9.1666
1000	8.8945	8.8976	8.9182	8.9820	9.2291
1200	8.9448	8.9478	8.9687	9.0333	9.2832
1400	8.9886	8.9917	9.0127	9.0780	9.3304
1600	9.0271	9.0302	9.0514	9.1172	9.3719
1800	9.0612	9.0644	9.0857	9.1520	9.4086

(3) Clamped at both ends:

$$\begin{aligned}
 u(0) = 0, \quad w(0) = 0, \quad \theta_x(0) = 0, \quad \phi_x(0) = 0, \quad \psi_x(0) = 0 \\
 u(L/2) = 0, \quad \theta_x(L/2) = 0, \quad \phi_x(L/2) = 0, \quad \psi_x(L/2) = 0
 \end{aligned}
 \quad (5.3)$$

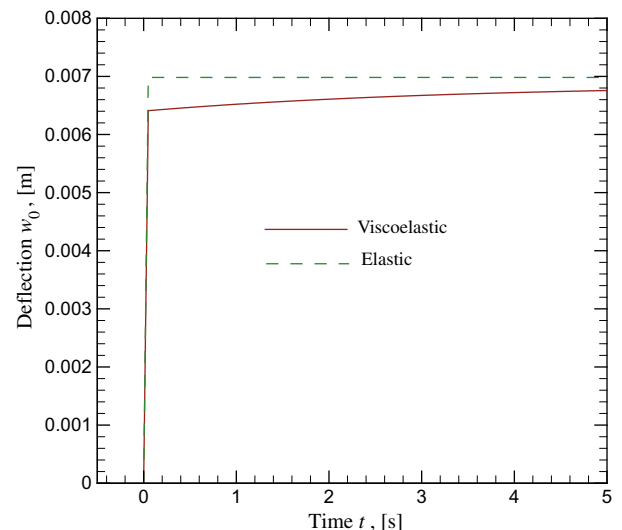
### 5.1. Quasi-static analysis of thin beams

In the first example, we compare the results for a thin isotropic beam ( $L/h > 20$ ) in  $x$  and  $z$  directions with the results presented in Ref. [18], for a  $n$ -parameter Kelvin-Voigt solid. The viscoelastic material model is based on the experimental findings of Lai and

**Fig. 3.** Quasi-static maximum vertical deflection  $w_{max}$ , of hinged-hinged beam under harmonic time-dependent transverse loading  $q(t)$ .

Bakker [29], for a glassy amorphous polymer material known as PMMA. The Prony series parameters for the viscoelastic relaxation modulus given in Table 1 were calculated by Payette and Reddy [17], from the published compliance parameters in Ref. [29]. Although the finite element formulation places no restriction on the relationship between  $E(t)$  and  $G(t)$ , for the present analysis we adopt the approach taken by Chen [30], and assume that the shear and relaxation moduli are related as  $G(t) = E(t)/2(1 + \nu)$ , where  $\nu$  is Poisson's ratio of the material, which is assumed to be time-independent and equal to  $\nu = 0.4$  [31].

A viscoelastic beam of uniform cross section  $1 \times 1$  in., and length  $L = 100$  in., with material properties given in Table 1 is used for the analysis. At  $t = 0$  the beam is subjected to a time invariant uniform vertical distributed load  $q = 0.25$  lb<sub>f</sub>/in. A constant time step  $\Delta t = 1.0$  s is employed with a total simulation time of 1800 s. Graphical results are presented in Fig. 2 for a beam discretized with two finite elements with 5th order spectral interpolation

**Fig. 4.** Quasi-static maximum vertical deflection  $w_{max}$ , of hinged-hinged elastic and viscoelastic beams under time-dependent transverse loading  $q(t)$ .



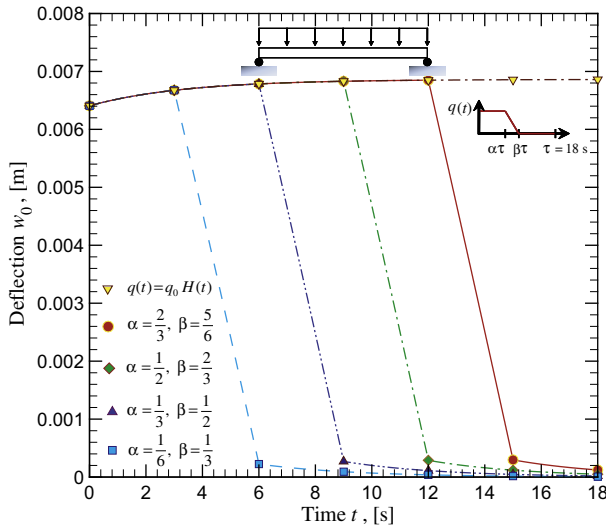


Fig. 5. Quasi-static maximum vertical deflection  $w_{max}$ , of hinged-hinged beam under heaviside time-dependent transverse loading  $q(t)$ .

functions. As expected, the deflection steadily increases, and then approaches a zero slope of equilibrium or a long-time constant value. This behavior is called creep under constant load. Also at  $t = 0$ , the results coincide with the instantaneous elastic solution, where Young's modulus is given as  $E = 535.4 \text{ Ksi}$ .

For the hinged-hinged beam configuration, the vertical deflection is compared with the following exact solution by Flügge [8], for a geometrically linear viscoelastic beam based on the Timoshenko beam theory

$$w_0(L/2, t) = \frac{5q_0 L^4}{384D_2} \left[ 1 + \frac{8(1+\nu)}{5K_s} \left( \frac{h}{L} \right)^2 \right] D(t) \quad (5.4)$$

where  $D(t)$  is the creep compliance and  $K_s$  is the shear correction factor. The results are given in Table 2 with different values of time steps  $\Delta t$ .

In the second example, we study the cyclic creep response of a thin orthotropic beam modeled as a Maxwell Solid. The values of elastic moduli taken from Johnson et al. [16], are  $E_x = 38.6 \text{ GPa}$ ,  $E_z = 8.27 \text{ GPa}$ ,  $G_{xz} = 4.14 \text{ GPa}$ ,  $\nu_{xz} = 0.26$ ,  $\nu_{zx} = \nu_{xz} E_z / E_x$  and the Prony series is taken as

$$P(t) = 1.0 + 0.01755e^{-0.0001t} + 0.000257e^{-0.01t} + 0.072014e^{-0.3162t} \quad (5.5)$$

The time dependent viscous relaxation moduli is taken as  $\mathbf{Q}(t) = \mathbf{Q}P(t)$ . A beam with dimensions, length  $L = 0.6 \text{ m}$ , height  $h = 0.02 \text{ m}$ , and base  $b = 0.01 \text{ m}$  is used for analysis. The beam is simply supported and is subjected to the following harmonic distributed load on the surface.

$$q(t) = 0, \quad t \leq 0$$

$$q(t) = q_0 \left[ \sin \left( \frac{\pi}{2\tau} t + \phi \right) \right], \quad t > 0 \quad (5.6)$$

where  $q_0 = 0.01 \text{ MPa}$ ,  $\tau = 0.04$  and  $\phi = 0$ . The beam is discretized using 40 finite elements with 3rd order spectral interpolation functions. A constant time step  $\Delta t = 0.001 \text{ s}$  is employed with a total simulation time of 1 s. In Fig. 3 we present the values of maximum vertical deflection of the beam. The oscillations in the maximum and minimum values demonstrate the cyclic creep behavior of the beam.

## 5.2. Quasi-static analysis of thick beams

In this example, we present numerical solutions for creep response of thick ( $L/h < 20$ ) orthotropic beam modeled as a Maxwell solid. The elastic moduli and the Prony series are the same as in the above example. The dimensions of the beam are length  $L = 0.1 \text{ m}$ , height  $h = 0.02 \text{ m}$ , and base  $b = 0.01 \text{ m}$ . The beam is simply supported and is subjected to a vertical distributed load on the top surface. The load is ramped from a value of 0.0–1.0 MPa in 0.05 s and is maintained constant for the rest of the time. A constant time step  $\Delta t = 0.01 \text{ s}$  is employed with a total simulation time of 5.0 s. The beam is discretized with 10 finite elements with 4th order spectral interpolation functions. The creep response is shown in Fig. 4, as expected both the elastic and viscous response converge over time.

Next, we investigate the elastic creep recovery behavior of the constitutive model using the following time dependent load for the same beam as above. An important characteristic is that the beam should eventually return to its original configuration once the loads are removed. To demonstrate that the present finite element model captures this effect, we consider a hinged-hinged beam subjected to the below quasi-static transverse load of intensity  $q_0$

$$q(t) = q_0 \left\{ H(t) - \frac{1}{\tau(\beta - \alpha)} [(t - \alpha\tau)H(t - \alpha\tau) - (t - \beta\tau)H(t - \beta\tau)] \right\} \quad (5.7)$$

where  $H(t)$  is the Heaviside function, and we take  $q_0 = 1.0 \text{ MPa}$  and  $\tau = 1800 \text{ s}$ . The parameters  $0 \leq \alpha \leq \beta \leq 1$  are constants. The Eq. (5.7) represents a load function that is constant in  $0 < t < \alpha\tau$  and then linearly decreases to zero from  $t = \alpha\tau$  to  $t = \beta\tau$ . For  $t > \beta\tau$ , the load is maintained at zero (see the inset in Fig. 5). A constant time step  $\Delta t = 0.01 \text{ s}$  is employed with a total simulation time of 18 s and the beam is discretized with 10 finite elements with 4th order spectral interpolation functions. In Fig. 5 we present the numerical results for various values of  $\alpha$  and  $\beta$ . As expected, each one of the curves in the figure follow a path of delayed recovery from  $t = \alpha\tau$  to  $t = \beta\tau$  and to their original configurations as time  $t$  gradually tends to infinity with the applied loads being removed.

## 6. Conclusions

In this paper a fully-discretized finite element model for an orthotropic, linear viscoelastic beam based on a general third-order beam theory has been developed. The 2-D plane-stress constitutive model is used for the viscoelastic formulation. The beam considered is capable of undergoing moderate rotations and small strains in the sense of the *von Kármán* geometric nonlinear strains. The assumed displacement field allows for a better bending-extensional coupling and the use of  $C^0$ -continuous functions for all the primary variables, thus simplifying the implementation. A two-point recurrence scheme is developed such that history from the last time step needs to be stored. Various numerical examples have been included to demonstrate the capabilities of the developed finite element model.

## Acknowledgments

The research reported herein was carried out while the first and third authors were supported by the MURI09 Project from the Air Force Office of Scientific Research under Grant FA9550-09-1-0686.

## Appendix A. Semi-discretized equations

In this Appendix we present explicitly the components of the semi-discretized finite element model.

$$\begin{aligned}
K_{ij}^{11} &= \int_{x_a}^{x_b} D_0 Q_{11}(0) \frac{\partial \psi_i}{\partial x} \frac{\partial \psi_j}{\partial x} dx, \quad K_{ij}^{12} = \int_{x_a}^{x_b} D_0 Q_{11}(0) \frac{1}{2} \frac{\partial w}{\partial x} \frac{\partial \psi_i}{\partial x} \frac{\partial \psi_j}{\partial x} dx \\
K_{ij}^{14} &= \int_{x_a}^{x_b} D_2 Q_{11}(0) \frac{\partial \psi_i}{\partial x} \frac{\partial \psi_j}{\partial x} dx, \quad K_{ij}^{16} = \int_{x_a}^{x_b} D_0 Q_{13}(0) \frac{\partial \psi_i}{\partial x} \psi_j dx \\
K_{ij}^{21} &= \int_{x_a}^{x_b} D_0 Q_{11}(0) \frac{\partial w}{\partial x} \frac{\partial \psi_i}{\partial x} \frac{\partial \psi_j}{\partial x} dx \\
K_{ij}^{22} &= \int_{x_a}^{x_b} D_0 Q_{11}(0) \frac{1}{2} \left( \frac{\partial w}{\partial x} \right)^2 \frac{\partial \psi_i}{\partial x} \frac{\partial \psi_j}{\partial x} dx + D_0 Q_{55}(0) \frac{\partial \psi_i}{\partial x} \frac{\partial \psi_j}{\partial x} dx \\
K_{ij}^{23} &= \int_{x_a}^{x_b} D_0 Q_{55}(0) \frac{\partial \psi_i}{\partial x} \psi_j dx, \quad K_{ij}^{24} = \int_{x_a}^{x_b} D_2 Q_{11}(0) \frac{\partial w}{\partial x} \frac{\partial \psi_i}{\partial x} \frac{\partial \psi_j}{\partial x} dx \\
K_{ij}^{25} &= \int_{x_a}^{x_b} D_2 Q_{55}(0) 3 \frac{\partial \psi_i}{\partial x} \psi_j dx, \quad K_{ij}^{26} = \int_{x_a}^{x_b} D_0 Q_{13}(0) \frac{\partial w}{\partial x} \frac{\partial \psi_i}{\partial x} \psi_j dx \\
K_{ij}^{27} &= \int_{x_a}^{x_b} D_2 Q_{55}(0) \frac{\partial \psi_i}{\partial x} \frac{\partial \psi_j}{\partial x} dx, \quad K_{ij}^{32} = \int_{x_a}^{x_b} D_0 Q_{55}(0) \psi_i \frac{\partial \psi_j}{\partial x} dx \\
K_{ij}^{33} &= \int_{x_a}^{x_b} D_2 Q_{11}(0) \frac{\partial \psi_i}{\partial x} \frac{\partial \psi_j}{\partial x} dx + D_0 Q_{55}(0) \psi_i \psi_j dx, \\
K_{ij}^{35} &= \int_{x_a}^{x_b} D_4 Q_{11}(0) \frac{\partial \psi_i}{\partial x} \frac{\partial \psi_j}{\partial x} dx + D_2 Q_{55}(0) 3 \psi_i \psi_j dx
\end{aligned} \tag{A.1}$$

where

$$D_i = \int_{A^e} z^i dA \tag{A.2}$$

$$\begin{aligned}
K_{ij}^{37} &= \int_{x_a}^{x_b} 2D_2 Q_{13}(0) \frac{\partial \psi_i}{\partial x} \psi_j dx + D_2 Q_{55}(0) \psi_i \frac{\partial \psi_j}{\partial x} dx \\
K_{ij}^{41} &= \int_{x_a}^{x_b} D_2 Q_{11}(0) \frac{\partial \psi_i}{\partial x} \frac{\partial \psi_j}{\partial x} dx, \quad K_{ij}^{42} = \int_{x_a}^{x_b} D_2 Q_{11}(0) \frac{1}{2} \frac{\partial w}{\partial x} \frac{\partial \psi_i}{\partial x} \frac{\partial \psi_j}{\partial x} dx \\
K_{ij}^{44} &= \int_{x_a}^{x_b} D_4 Q_{11}(0) \frac{\partial \psi_i}{\partial x} \frac{\partial \psi_j}{\partial x} dx + 2D_2 Q_{55}(0) 2 \psi_i \psi_j dx \\
K_{ij}^{46} &= \int_{x_a}^{x_b} D_2 Q_{13}(0) \frac{\partial \psi_i}{\partial x} \psi_j dx + 2D_2 Q_{55}(0) \psi_i \frac{\partial \psi_j}{\partial x} dx \\
K_{ij}^{52} &= \int_{x_a}^{x_b} 3D_2 Q_{55}(0) \psi_i \frac{\partial \psi_j}{\partial x} dx \\
K_{ij}^{53} &= \int_{x_a}^{x_b} D_4 Q_{11}(0) \frac{\partial \psi_i}{\partial x} \frac{\partial \psi_j}{\partial x} dx + 3D_2 Q_{55}(0) \psi_i \psi_j dx, \\
K_{ij}^{55} &= \int_{x_a}^{x_b} D_6 Q_{11}(0) \frac{\partial \psi_i}{\partial x} \frac{\partial \psi_j}{\partial x} dx + 9D_4 Q_{55}(0) \psi_i \psi_j dx \\
K_{ij}^{57} &= \int_{x_a}^{x_b} 2D_4 Q_{13}(0) \frac{\partial \psi_i}{\partial x} \psi_j dx + 3D_4 Q_{55}(0) \psi_i \frac{\partial \psi_j}{\partial x} dx \\
K_{ij}^{61} &= \int_{x_a}^{x_b} D_0 Q_{13}(0) \psi_i \frac{\partial \psi_j}{\partial x} dx, \quad K_{ij}^{62} = \int_{x_a}^{x_b} D_0 Q_{13}(0) \frac{1}{2} \frac{\partial w}{\partial x} \psi_i \frac{\partial \psi_j}{\partial x} dx \\
K_{ij}^{64} &= \int_{x_a}^{x_b} D_2 Q_{55}(0) 2 \frac{\partial \psi_i}{\partial x} \psi_j dx + D_2 Q_{13}(0) \psi_i \frac{\partial \psi_j}{\partial x} dx \\
K_{ij}^{66} &= \int_{x_a}^{x_b} D_2 Q_{55}(0) \frac{\partial \psi_i}{\partial x} \frac{\partial \psi_j}{\partial x} dx + D_0 Q_{33}(0) \psi_i \psi_j dx \\
K_{ij}^{72} &= \int_{x_a}^{x_b} D_2 Q_{55}(0) \frac{\partial \psi_i}{\partial x} \frac{\partial \psi_j}{\partial x} dx \\
K_{ij}^{73} &= \int_{x_a}^{x_b} D_2 Q_{55}(0) \frac{\partial \psi_i}{\partial x} \psi_j dx + 2D_2 Q_{13}(0) \psi_i \frac{\partial \psi_j}{\partial x} dx \\
K_{ij}^{75} &= \int_{x_a}^{x_b} D_4 Q_{55}(0) 3 \frac{\partial \psi_i}{\partial x} \psi_j dx + 2D_4 Q_{13}(0) \psi_i \frac{\partial \psi_j}{\partial x} dx \\
K_{ij}^{77} &= \int_{x_a}^{x_b} D_4 Q_{55}(0) \frac{\partial \psi_i}{\partial x} \frac{\partial \psi_j}{\partial x} dx + 4D_2 Q_{33}(0) \psi_i \psi_j dx
\end{aligned} \tag{A.3}$$

$$\begin{aligned}
\tilde{K}_{ij}^{11} &= \int_{x_a}^{x_b} D_0 \dot{Q}_{11}(t-s) \frac{\partial \psi_i}{\partial x} \frac{\partial \psi_j}{\partial x} dx, \quad \tilde{K}_{ij}^{12} = \int_{x_a}^{x_b} D_0 \dot{Q}_{11}(t-s) \frac{1}{2} \frac{\partial w(x,s)}{\partial x} \frac{\partial \psi_i}{\partial x} \frac{\partial \psi_j}{\partial x} dx \\
\tilde{K}_{ij}^{14} &= \int_{x_a}^{x_b} D_2 \dot{Q}_{11}(t-s) \frac{\partial \psi_i}{\partial x} \frac{\partial \psi_j}{\partial x} dx, \quad \tilde{K}_{ij}^{16} = \int_{x_a}^{x_b} D_0 \dot{Q}_{13}(t-s) \frac{\partial \psi_i}{\partial x} \psi_j dx \\
\tilde{K}_{ij}^{21} &= \int_{x_a}^{x_b} D_0 \dot{Q}_{11}(t-s) \frac{\partial w}{\partial x} \frac{\partial \psi_i}{\partial x} \frac{\partial \psi_j}{\partial x} dx \\
\tilde{K}_{ij}^{22} &= \int_{x_a}^{x_b} D_0 \dot{Q}_{11}(t-s) \frac{1}{2} \frac{\partial w(x,s)}{\partial x} \frac{\partial w}{\partial x} \frac{\partial \psi_i}{\partial x} \frac{\partial \psi_j}{\partial x} dx + D_0 \dot{Q}_{55}(t-s) \frac{\partial \psi_i}{\partial x} \frac{\partial \psi_j}{\partial x} dx \\
\tilde{K}_{ij}^{23} &= \int_{x_a}^{x_b} D_0 \dot{Q}_{55}(t-s) \frac{\partial \psi_i}{\partial x} \psi_j dx, \quad \tilde{K}_{ij}^{24} = \int_{x_a}^{x_b} D_2 \dot{Q}_{11}(t-s) \frac{\partial w}{\partial x} \frac{\partial \psi_i}{\partial x} \frac{\partial \psi_j}{\partial x} dx \\
\tilde{K}_{ij}^{25} &= \int_{x_a}^{x_b} D_2 \dot{Q}_{55}(t-s) 3 \frac{\partial \psi_i}{\partial x} \psi_j dx \\
\tilde{K}_{ij}^{26} &= \int_{x_a}^{x_b} D_0 \dot{Q}_{13}(t-s) \frac{\partial w}{\partial x} \frac{\partial \psi_i}{\partial x} \psi_j dx, \quad \tilde{K}_{ij}^{27} = \int_{x_a}^{x_b} D_2 \dot{Q}_{55}(t-s) \frac{\partial \psi_i}{\partial x} \frac{\partial \psi_j}{\partial x} dx \\
\tilde{K}_{ij}^{32} &= \int_{x_a}^{x_b} D_0 \dot{Q}_{55}(t-s) \psi_i \frac{\partial \psi_j}{\partial x} dx \\
\tilde{K}_{ij}^{33} &= \int_{x_a}^{x_b} D_2 \dot{Q}_{11}(t-s) \frac{\partial \psi_i}{\partial x} \frac{\partial \psi_j}{\partial x} dx + D_0 \dot{Q}_{55}(t-s) \psi_i \psi_j dx, \\
\tilde{K}_{ij}^{35} &= \int_{x_a}^{x_b} D_4 \dot{Q}_{11}(t-s) \frac{\partial \psi_i}{\partial x} \frac{\partial \psi_j}{\partial x} dx + D_2 \dot{Q}_{55}(t-s) 3 \psi_i \psi_j dx \\
\tilde{K}_{ij}^{37} &= \int_{x_a}^{x_b} 2D_2 \dot{Q}_{13}(t-s) \frac{\partial \psi_i}{\partial x} \psi_j dx + D_2 \dot{Q}_{55}(t-s) \psi_i \frac{\partial \psi_j}{\partial x} dx \\
\tilde{K}_{ij}^{41} &= \int_{x_a}^{x_b} D_2 \dot{Q}_{11}(t-s) \frac{\partial \psi_i}{\partial x} \frac{\partial \psi_j}{\partial x} dx \\
\tilde{K}_{ij}^{42} &= \int_{x_a}^{x_b} D_2 \dot{Q}_{11}(t-s) \frac{1}{2} \frac{\partial w(x,s)}{\partial x} \frac{\partial \psi_i}{\partial x} \frac{\partial \psi_j}{\partial x} dx
\end{aligned} \tag{A.4}$$

$$\begin{aligned}
\tilde{K}_{ij}^{44} &= \int_{x_a}^{x_b} D_4 \dot{Q}_{11}(t-s) \frac{\partial \psi_i}{\partial x} \frac{\partial \psi_j}{\partial x} dx + 2D_2 \dot{Q}_{55}(t-s) 2 \psi_i \psi_j dx \\
\tilde{K}_{ij}^{46} &= \int_{x_a}^{x_b} D_2 \dot{Q}_{13}(t-s) \frac{\partial \psi_i}{\partial x} \psi_j dx + 2D_2 \dot{Q}_{55}(t-s) \psi_i \frac{\partial \psi_j}{\partial x} dx \\
\tilde{K}_{ij}^{52} &= \int_{x_a}^{x_b} 3D_2 \dot{Q}_{55}(t-s) \psi_i \frac{\partial \psi_j}{\partial x} dx \\
\tilde{K}_{ij}^{53} &= \int_{x_a}^{x_b} D_4 \dot{Q}_{11}(t-s) \frac{\partial \psi_i}{\partial x} \frac{\partial \psi_j}{\partial x} dx + 3D_2 \dot{Q}_{55}(t-s) \psi_i \psi_j dx, \\
\tilde{K}_{ij}^{55} &= \int_{x_a}^{x_b} D_6 \dot{Q}_{11}(t-s) \frac{\partial \psi_i}{\partial x} \frac{\partial \psi_j}{\partial x} dx + 9D_4 \dot{Q}_{55}(t-s) \psi_i \psi_j dx \\
\tilde{K}_{ij}^{57} &= \int_{x_a}^{x_b} 2D_4 \dot{Q}_{13}(t-s) \frac{\partial \psi_i}{\partial x} \psi_j dx + 3D_4 \dot{Q}_{55}(t-s) \psi_i \frac{\partial \psi_j}{\partial x} dx \\
\tilde{K}_{ij}^{61} &= \int_{x_a}^{x_b} D_0 \dot{Q}_{13}(t-s) \psi_i \frac{\partial \psi_j}{\partial x} dx, \quad \tilde{K}_{ij}^{62} = \int_{x_a}^{x_b} D_0 \dot{Q}_{13}(0) \frac{1}{2} \frac{\partial w(x,s)}{\partial x} \psi_i \frac{\partial \psi_j}{\partial x} dx \\
\tilde{K}_{ij}^{64} &= \int_{x_a}^{x_b} D_2 \dot{Q}_{55}(t-s) 2 \frac{\partial \psi_i}{\partial x} \psi_j dx + D_2 \dot{Q}_{13}(t-s) \psi_i \frac{\partial \psi_j}{\partial x} dx \\
\tilde{K}_{ij}^{66} &= \int_{x_a}^{x_b} D_2 \dot{Q}_{55}(t-s) \frac{\partial \psi_i}{\partial x} \frac{\partial \psi_j}{\partial x} dx + D_0 \dot{Q}_{33}(t-s) \psi_i \psi_j dx \\
\tilde{K}_{ij}^{72} &= \int_{x_a}^{x_b} D_2 \dot{Q}_{55}(t-s) \frac{\partial \psi_i}{\partial x} \frac{\partial \psi_j}{\partial x} dx \\
\tilde{K}_{ij}^{73} &= \int_{x_a}^{x_b} D_2 \dot{Q}_{55}(t-s) \frac{\partial \psi_i}{\partial x} \psi_j dx + 2D_2 \dot{Q}_{13}(t-s) \psi_i \frac{\partial \psi_j}{\partial x} dx \\
\tilde{K}_{ij}^{75} &= \int_{x_a}^{x_b} D_4 \dot{Q}_{55}(t-s) 3 \frac{\partial \psi_i}{\partial x} \psi_j dx + 2D_4 \dot{Q}_{13}(t-s) \psi_i \frac{\partial \psi_j}{\partial x} dx \\
\tilde{K}_{ij}^{77} &= \int_{x_a}^{x_b} D_4 \dot{Q}_{55}(t-s) \frac{\partial \psi_i}{\partial x} \frac{\partial \psi_j}{\partial x} dx + 4D_2 \dot{Q}_{33}(t-s) \psi_i \psi_j dx
\end{aligned} \tag{A.5}$$

All other stiffness coefficients are zero.

## Appendix B. Fully-discretized equations and tangent matrix

### B.1. Fully-discretized finite element equations

The additional matrices introduced in the fully-discretized form of the finite element equations can be expressed as



[illegible]

$$\begin{aligned}
\bar{K}_{ij}^{64} &= \int_{x_a}^{x_b} D_2 \left( Q_{55}(0) + \frac{\Delta t_{N-1}}{2} \dot{Q}_{55}(0) \right) 2 \frac{\partial \psi_i}{\partial x} \psi_j dx + D_2 \left( Q_{13}(0) + \frac{\Delta t_{N-1}}{2} \dot{Q}_{13}(0) \right) \psi_i \frac{\partial \psi_j}{\partial x}, \\
\bar{K}_{ij}^{66} &= \int_{x_a}^{x_b} D_2 \left( Q_{55}(0) + \frac{\Delta t_{N-1}}{2} \dot{Q}_{55}(0) \right) \frac{\partial \psi_i}{\partial x} \frac{\partial \psi_j}{\partial x} dx + D_0 \left( Q_{33}(0) + \frac{\Delta t_{N-1}}{2} \dot{Q}_{33}(0) \right) \psi_i \psi_j dx \\
\bar{K}_{ij}^{72} &= \int_{x_a}^{x_b} D_2 \left( Q_{55}(0) + \frac{\Delta t_{N-1}}{2} \dot{Q}_{55}(0) \right) \frac{\partial \psi_i}{\partial x} \frac{\partial \psi_j}{\partial x} dx, \\
\bar{K}_{ij}^{73} &= \int_{x_a}^{x_b} D_2 \left( Q_{55}(0) + \frac{\Delta t_{N-1}}{2} \dot{Q}_{55}(0) \right) \frac{\partial \psi_i}{\partial x} \psi_j dx + 2D_2 \left( Q_{13}(0) + \frac{\Delta t_{N-1}}{2} \dot{Q}_{13}(0) \right) \psi_i \frac{\partial \psi_j}{\partial x} dx \\
\bar{K}_{ij}^{75} &= \int_{x_a}^{x_b} D_4 \left( Q_{55}(0) + \frac{\Delta t_{N-1}}{2} \dot{Q}_{55}(0) \right) 3 \frac{\partial \psi_i}{\partial x} \psi_j dx + 2D_4 \left( Q_{13}(0) + \frac{\Delta t_{N-1}}{2} \dot{Q}_{13}(0) \right) \psi_i \frac{\partial \psi_j}{\partial x} dx, \\
\bar{K}_{ij}^{77} &= \int_{x_a}^{x_b} D_4 \left( Q_{55}(0) + \frac{\Delta t_{N-1}}{2} \dot{Q}_{55}(0) \right) \frac{\partial \psi_i}{\partial x} \frac{\partial \psi_j}{\partial x} dx + 4D_2 \left( Q_{33}(0) + \frac{\Delta t_{N-1}}{2} \dot{Q}_{33}(0) \right) \psi_i \psi_j dx
\end{aligned} \quad (B.2)$$

All other terms are zeros. The specific forms of the viscoelastic force vector  $\tilde{Q}$  in Eq. (4.7) and the history terms  $\bar{X}_i^{lm}(t_N)$  appearing in it are not provided due to space constraints; the derivation of these components is similar to the one shown in Ref. [18].

## B.2. Tangent stiffness matrix

The fully discretized finite element equations are nonlinear due to inclusion of the *von Kármán* strains in the formulation. For our formulation we solve the equations iteratively using Newton–Raphson linearization procedure [32]. The linearized equations are of the form

$$\begin{aligned}
\{\Delta^{(r)}\}_s &= \{\Delta^{(r-1)}\}_s \\
&\quad - [\bar{T}]_s^{-1} \left( [\bar{K}]^{(r-1)}_s \{\Delta^{(r-1)}\}_s + \{F^{(r-1)}\}_s - \{\tilde{Q}^{(r-1)}\}_s \right)
\end{aligned} \quad (B.3)$$

where  $\{\Delta^{(r)}\}_s$  represents the solution at the  $r$ 'th iteration and time  $t = t_s$ . The tangent stiffness matrix  $[\bar{T}]_s$  in Eq. (B.3) is defined using Einstein's summation notation as

$$\bar{T}_{ij} = \sum_1^n \bar{K}_{ij} + \frac{\partial \bar{K}_{im}}{\partial \Delta_j} \Delta_m + \frac{\partial \tilde{Q}_i}{\partial \Delta_j} \quad (B.4)$$

All quantities in Eq. (B.4) comprising the tangent stiffness matrix are formulated using the solution from  $(r-1)$ 'th iteration. It is important to note that all the partial derivatives are taken with respect to the solution of the current time step. Applying the Newton's method to the fully-discretized beam equations results in the following components of tangent stiffness matrix

$$\bar{T}_{ij}^{11} = \bar{K}_{ij}^{11}, \quad \bar{T}_{ij}^{12} = 2\bar{K}_{ij}^{12}, \quad \bar{T}_{ij}^{14} = \bar{K}_{ij}^{14}, \quad \bar{T}_{ij}^{16} = \bar{K}_{ij}^{16} \quad (B.5)$$

$$\bar{T}_{ij}^{21} = \bar{K}_{ij}^{21},$$

$$\begin{aligned}
\bar{T}_{ij}^{22} &= \bar{K}_{ij}^{22} + \int_{x_a}^{x_b} D_0 \left( Q_{11}(0) + \frac{\Delta t_{N-1}}{2} \dot{Q}_{11}(0) \right) \frac{\partial u}{\partial x} \frac{\partial \psi_i}{\partial x} \frac{\partial \psi_j}{\partial x} dx \\
&\quad + \int_{x_a}^{x_b} D_0 \left( Q_{11}(0) + \frac{\Delta t_{N-1}}{2} \dot{Q}_{11}(0) \right) \left( \frac{\partial w}{\partial x} \right)^2 \frac{\partial \psi_i}{\partial x} \frac{\partial \psi_j}{\partial x} dx \\
&\quad + \int_{x_a}^{x_b} D_2 \left( Q_{11}(0) + \frac{\Delta t_{N-1}}{2} \dot{Q}_{11}(0) \right) \frac{\partial \phi_x}{\partial x} \frac{\partial \psi_i}{\partial x} \frac{\partial \psi_j}{\partial x} dx \\
&\quad + \int_{x_a}^{x_b} D_0 \left( Q_{13}(0) + \frac{\Delta t_{N-1}}{2} \dot{Q}_{13}(0) \right) \frac{\partial \psi_i}{\partial x} \frac{\partial \psi_j}{\partial x} \theta_z dx \\
&\quad + \frac{\Delta t_{N-1}}{2} \int_{x_a}^{x_b} \dot{Q}_{11}(\Delta t_{N-1}) D_0 \frac{\partial u(x, t_{N-1})}{\partial x} \frac{\partial \psi_i}{\partial x} \frac{\partial \psi_j}{\partial x} dx
\end{aligned}$$

$$\begin{aligned}
&\quad + \sum_{l=1}^n \sum_{m=1}^{NGP} e^{-\frac{\Delta t_{N-1}}{\tau_{ix}^{lx}}} {}^5\bar{X}_i^{lm}(t_{N-1}) \frac{\partial \psi_j(x_m)}{\partial x} \\
&\quad + \frac{\Delta t_{N-1}}{2} \int_{x_a}^{x_b} \dot{Q}_{11}(\Delta t_{N-1}) D_0 \frac{1}{2} \left( \frac{\partial w(x, t_{N-1})}{\partial x} \right)^2 \frac{\partial \psi_i}{\partial x} \frac{\partial \psi_j}{\partial x} dx \\
&\quad + \sum_{l=1}^n \sum_{m=1}^{NGP} e^{-\frac{\Delta t_{N-1}}{\tau_{ix}^{lx}}} \frac{\partial \psi_j(x_m)}{\partial x} {}^6\bar{X}_i^{lm}(t_{N-1}) \\
&\quad + \frac{\Delta t_{N-1}}{2} \int_{x_a}^{x_b} \dot{Q}_{11}(\Delta t_{N-1}) D_2 \frac{\partial \phi_x(x, t_{N-1})}{\partial x} \frac{\partial \psi_i}{\partial x} \frac{\partial \psi_j}{\partial x} dx \\
&\quad + \sum_{l=1}^n \sum_{m=1}^{NGP} e^{-\frac{\Delta t_{N-1}}{\tau_{ix}^{lx}}} \frac{\partial \psi_j(x_m)}{\partial x} {}^9\bar{X}_i^{lm}(t_{N-1}) \\
&\quad + \frac{\Delta t_{N-1}}{2} \int_{x_a}^{x_b} \dot{Q}_{13}(\Delta t_{N-1}) D_0 \theta_z(x, t_{N-1}) \frac{\partial \psi_i}{\partial x} \frac{\partial \psi_j}{\partial x} dx \\
&\quad + \sum_{l=1}^n \sum_{m=1}^{NGP} e^{-\frac{\Delta t_{N-1}}{\tau_{ix}^{lx}}} \frac{\partial \psi_j(x_m)}{\partial x} {}^{11}\bar{X}_i^{lm}(t_{N-1}) \\
\bar{T}_{ij}^{23} &= \bar{K}_{ij}^{23}, \quad \bar{T}_{ij}^{24} = \bar{K}_{ij}^{24}, \quad \bar{T}_{ij}^{25} = \bar{K}_{ij}^{25}, \quad \bar{T}_{ij}^{26} = \bar{K}_{ij}^{26}, \quad \bar{T}_{ij}^{27} = \bar{K}_{ij}^{27} \quad (B.6)
\end{aligned}$$

$$\bar{T}_{ij}^{32} = \bar{K}_{ij}^{32}, \quad \bar{T}_{ij}^{33} = \bar{K}_{ij}^{33}, \quad \bar{T}_{ij}^{35} = \bar{K}_{ij}^{35}, \quad \bar{T}_{ij}^{37} = \bar{K}_{ij}^{37} \quad (B.7)$$

$$\bar{T}_{ij}^{41} = \bar{K}_{ij}^{41}, \quad \bar{T}_{ij}^{42} = 2\bar{K}_{ij}^{42}, \quad \bar{T}_{ij}^{44} = \bar{K}_{ij}^{44}, \quad \bar{T}_{ij}^{46} = \bar{K}_{ij}^{46} \quad (B.8)$$

$$\bar{T}_{ij}^{52} = \bar{K}_{ij}^{52}, \quad \bar{T}_{ij}^{53} = \bar{K}_{ij}^{53}, \quad \bar{T}_{ij}^{55} = \bar{K}_{ij}^{55}, \quad \bar{T}_{ij}^{57} = \bar{K}_{ij}^{57} \quad (B.9)$$

$$\bar{T}_{ij}^{61} = \bar{K}_{ij}^{61}, \quad \bar{T}_{ij}^{62} = 2\bar{K}_{ij}^{62}, \quad \bar{T}_{ij}^{64} = \bar{K}_{ij}^{64}, \quad \bar{T}_{ij}^{66} = \bar{K}_{ij}^{66} \quad (B.10)$$

$$\bar{T}_{ij}^{72} = \bar{K}_{ij}^{72}, \quad \bar{T}_{ij}^{73} = \bar{K}_{ij}^{73}, \quad \bar{T}_{ij}^{77} = \bar{K}_{ij}^{77} \quad (B.11)$$

## References

- [1] Christensen RM. Theory of viscoelasticity. 2nd ed. New York: Academic Press; 1982.
- [2] Gurtin ME, Sternberg E. On linear theory of viscoelasticity. Arch Rational Mech Anal 1962;11:291–356.
- [3] Findley WN, Lai JS, Onaran K. Creep and relaxation of nonlinear viscoelastic materials. New York: North-Holland Publishing Company; 1976.
- [4] Lockett FJ. Nonlinear viscoelastic solids. London: Academic Press; 1975.
- [5] Lakes RS. Viscoelastic materials. 1st ed. New York: Cambridge University Press; 2009.
- [6] Golden JM, Graham GAC. Boundary value problems in linear viscoelasticity. Berlin: Springer-Verlag; 1988.
- [7] Reddy JN. An introduction to continuum mechanics with applications. New York: Cambridge University Press; 2008.
- [8] Flügge W. Viscoelasticity. 2nd ed. Berlin (Heidelberg): Springer; 1975.
- [9] Reddy JN. An introduction to the finite element method. 3rd ed. New York: McGraw-Hill; 2006.
- [10] Brebbia CA, Telles JCF, Wrobel LC. Boundary element techniques. New York: Springer-verlag; 1984.

- [11] Yang TY, Lianis G. Large displacement analysis of viscoelastic beams and frames by the finite element method. *J Appl Mech* 1974;41:635–40.
- [12] Yagawa G, Miuzaki N, Ando Y. Superposition method of finite element and analytical solutions for transient creep analysis. *Int J Numer Methods Eng* 1977;11:1107–15.
- [13] Chen WH, Lin TC. Dynamic analysis of viscoelastic structures using incremental finite element method. *Eng. Struct.* 1982;4(4):271–6.
- [14] Coleman BD, Noll W. Foundations of linear viscoelasticity. *Rev Mod Phys* 1982;33(2):239–49.
- [15] Schapery RA, Noll W. Viscoelastic behavior and analysis of composite materials. *Compos Mater* 1974;2(2).
- [16] Johnson AR, Tessler A, Dambach R. Dynamics of thick viscoelastic beams. *J Eng Mater Technol* 1997;119:273–8.
- [17] Payette GS, Reddy JN. Nonlinear quasi-static finite element formulations for viscoelastic Euler–Bernoulli and Timoshenko beams. *Commun Numer Methods Eng* 2010;26(12):1736–55.
- [18] Vallala VP, Payette GS, Reddy JN. A spectral/hp finite element formulation for viscoelastic beams based on a high-order beam theory. *Int J Appl Mech* 2011;4(1):43–57.
- [19] Schapery RA. Stress analysis of viscoelastic composite materials. *J Compos Mater* 1967;1:228–67.
- [20] Halpin JC, Pagano NJ. Observations on linear anisotropic viscoelasticity. *J Compos Mater* 1968;2:68–80.
- [21] Schniewind AP, Barrett JD. Wood as a linear orthotropic viscoelastic material. *Wood Sci Technol* 1972;6:43–57.
- [22] Reddy JN. On locking-free shear deformable beam finite elements. *Commun Numer Methods Eng* 1997;149:113–32.
- [23] Reddy JN. Energy principles and variational methods in applied mechanics. 2nd ed. New York: John Wiley; 2002.
- [24] Reddy JN. An introduction to nonlinear finite element analysis. Oxford: Oxford University Press; 2004.
- [25] Pontaza JP. Least-squares variational principles and finite element method: theory, formulations, and models for solid and fluid mechanics. Ph.D. Thesis, College Station: Texas A& M University; 2003.
- [26] Karniadakis GE, Sherwin SJ. Spectral/hp element methods for computational fluid dynamics. Oxford: Oxford University Press; 2005.
- [27] Oden JT, Armstrong WH. Analysis of nonlinear dynamic coupled thermoviscoelasticity problems by the finite element method. *Comput Struct* 1971;1:603–21.
- [28] Simo JC, Hughes TJR. Computational inelasticity. 3rd ed. Berlin: Springer; 1998.
- [29] Lai J, Bakker A. 3-D schapery representation for non-linear viscoelasticity and finite element implementation. *Comput Mech* 1996;18:182–91.
- [30] Chen TM. The hybrid Laplace transform/finite element method applied to the quasi-static and dynamic analysis of viscoelastic Timoshenko beams. *Int J Numer Methods Eng* 1995;38(1):509–22.
- [31] Van Krevelen DW. Properties of polymers. 3rd ed. Amsterdam: Elsevier; 1990.
- [32] Bell BC, Surana KS. A space-time coupled *p*-version least-squares finite element formulation for unsteady two-dimensional Navier–Stokes equations. *Int J Numer Methods Eng* 1994;39:2593–618.